Supplementary Material

Rapid and Simultaneous Multiple Detection of a Tripledemic Using a Dual-gate Oxide Semiconductor Thin-film Transistor-based Immunosensor

Sehun Jeong†, Seong Uk Son†, Jingyu Kim, Seong-In Cho, Taejoon Kang, Sunjoo Kim, Eun-Kyung Lim, and Sang-Hee Ko Park**

Supplementary Table

Table S1. Immunosensor comparison of the limit of detection (LOD) among various types of FET-based immunosensors for influenza A pH1N1, SARS-CoV-2, and RSV.

Type of FET	Target	LOD	Ref.
Mxene-graphene FET	Influenza A pH1N1 HA	125 copies/mL	(Li et al., 2021)
Dual-channel FET	Influenza A pH1N1	$10^{0.5}$ $TCID_{50}$/mL	(Hideshima et al., 2019)
SiNW FET	Influenza A Hemagglutinin 1 domain	1 fM	(Uhm et al., 2019)
CNT-FET	SARS-CoV-2 S1	4.12 fg/mL	(Zamzami et al., 2022)
Remote floating-gate FET	SARS-CoV-2 S proteins	Few pg/mL	(Jang et al., 2022)
In_2O_3 nanoribbon transistor	SARS-CoV-2 S1	100 fg/mL	(Jang et al., 2022)
Transition metal dichalcogenide (TMDC)-based 2D FET	SARS-CoV-2 S proteins	25 fg/μL	(Fathi-Hafshejani et al., 2021)
MXene-graphene FET	SARS-CoV-2 S proteins	1 fg/mL	(Li et al., 2021)
Graphene FET	Nucleic acid target sequence of RSV	1 aM	(Li et al., 2022)
Dual-gate oxide FET	Influenza A pH1N1 HA	1.26 fg/mL	This study
Dual-gate oxide FET	SARS-CoV-2 S1	1.21 fg/mL	This study
Dual-gate oxide FET	RSV fusion	1.20 fg/mL	This study

Supplementary Figures

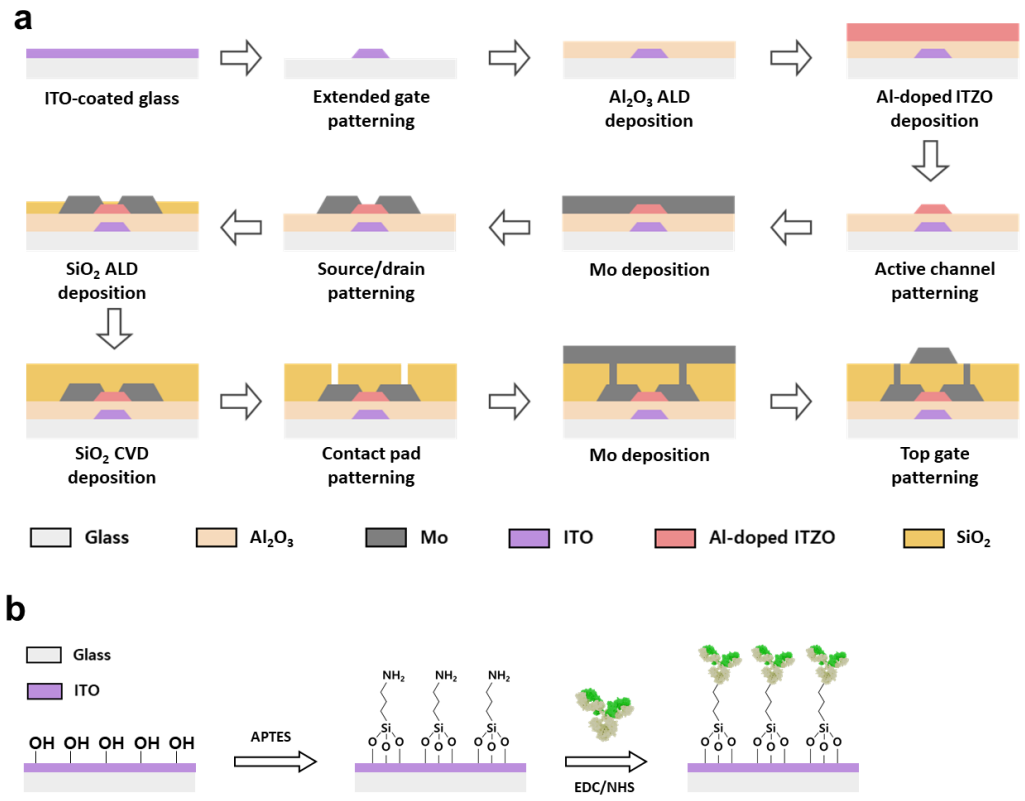

Figure S1. Schematic illustration of (a) TFT fabrication and (b) antibody immobilization.

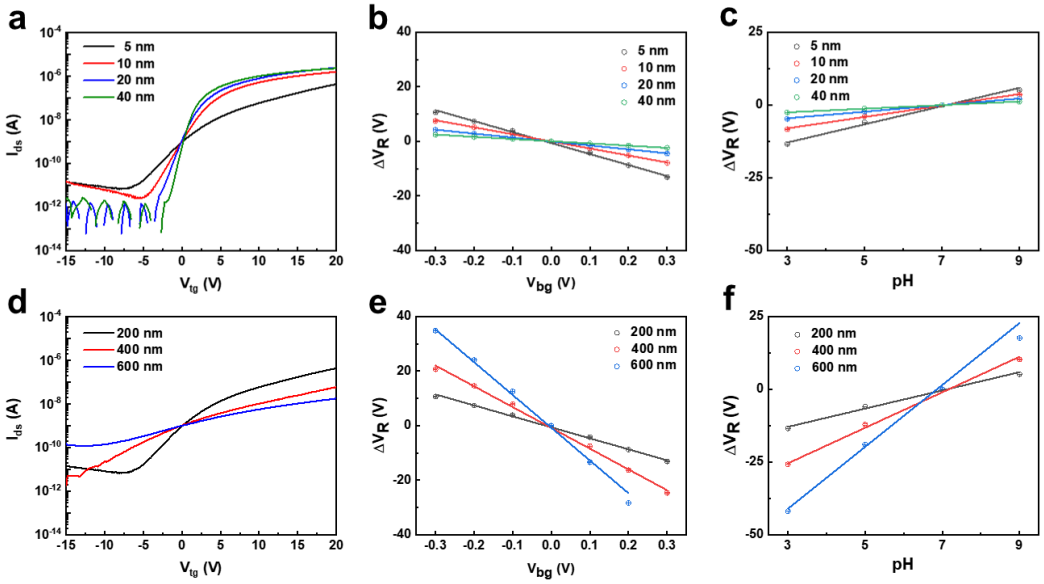

Figure S2. Transfer characteristic comparisons for modification of (a) bottom gate insulator (GI) and (d) top GI. Reference voltage changes by a constant bias on the bottom gate with modification of the (b) bottom and (e) top GI. Reference voltage changes by the standard buffer solution with modification of the (c) bottom and (f) top GI.

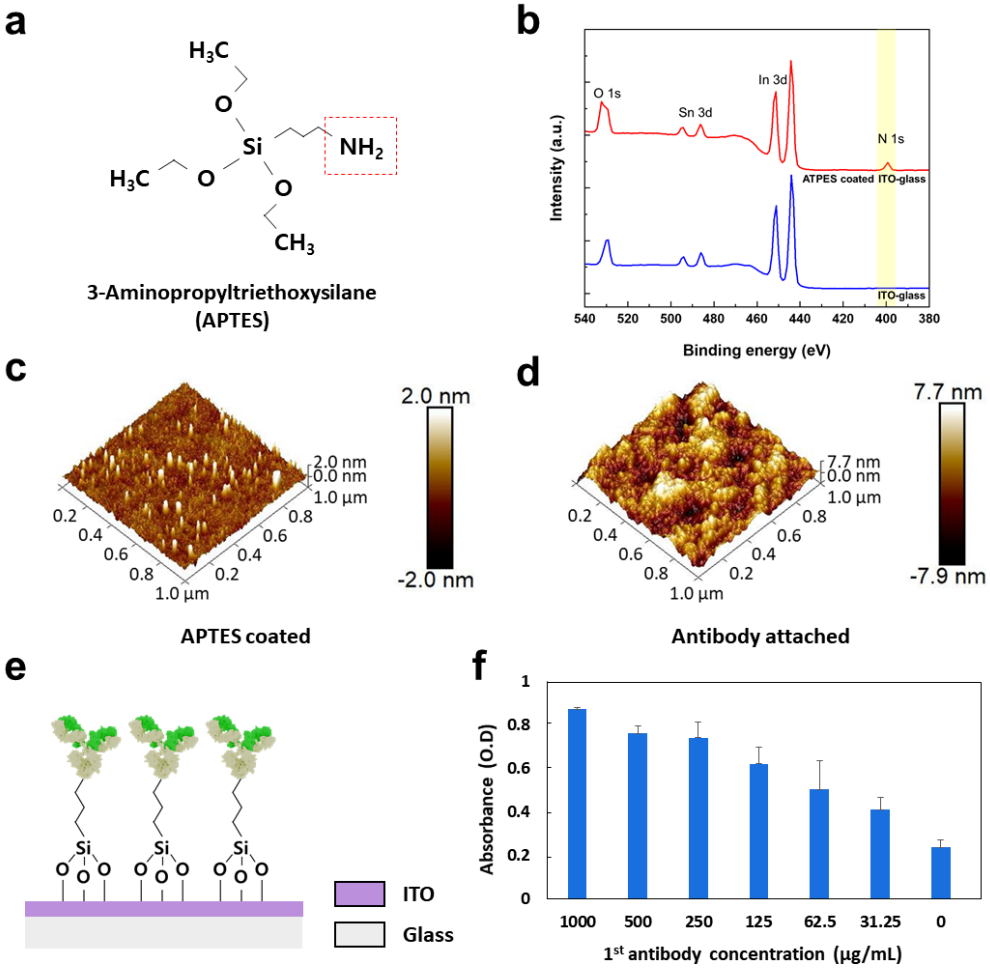

Figure S3. (a) Structure of APTES. (b) XPS spectra of ITO-glass (blue line) and APTES-coated ITO-glass (red line). (c) AFM image of APTES-coated glass and (d) antibody-coated glass. (e) Schematic diagram of antibody conjugated to the ITO-coated glass substrate. (f) Direct ELISA results of APTES-coated ITO-glass treated with antibodies.

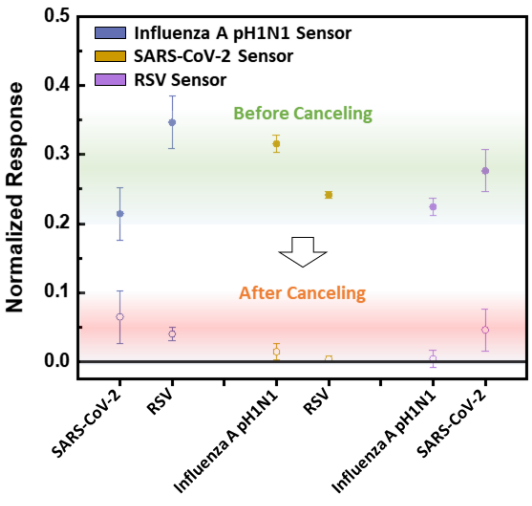

Figure S4. Normalized response to high-concentration sample detection before canceling (real-time current changes divided by initial current values in main sensor) and after canceling (normalized response).

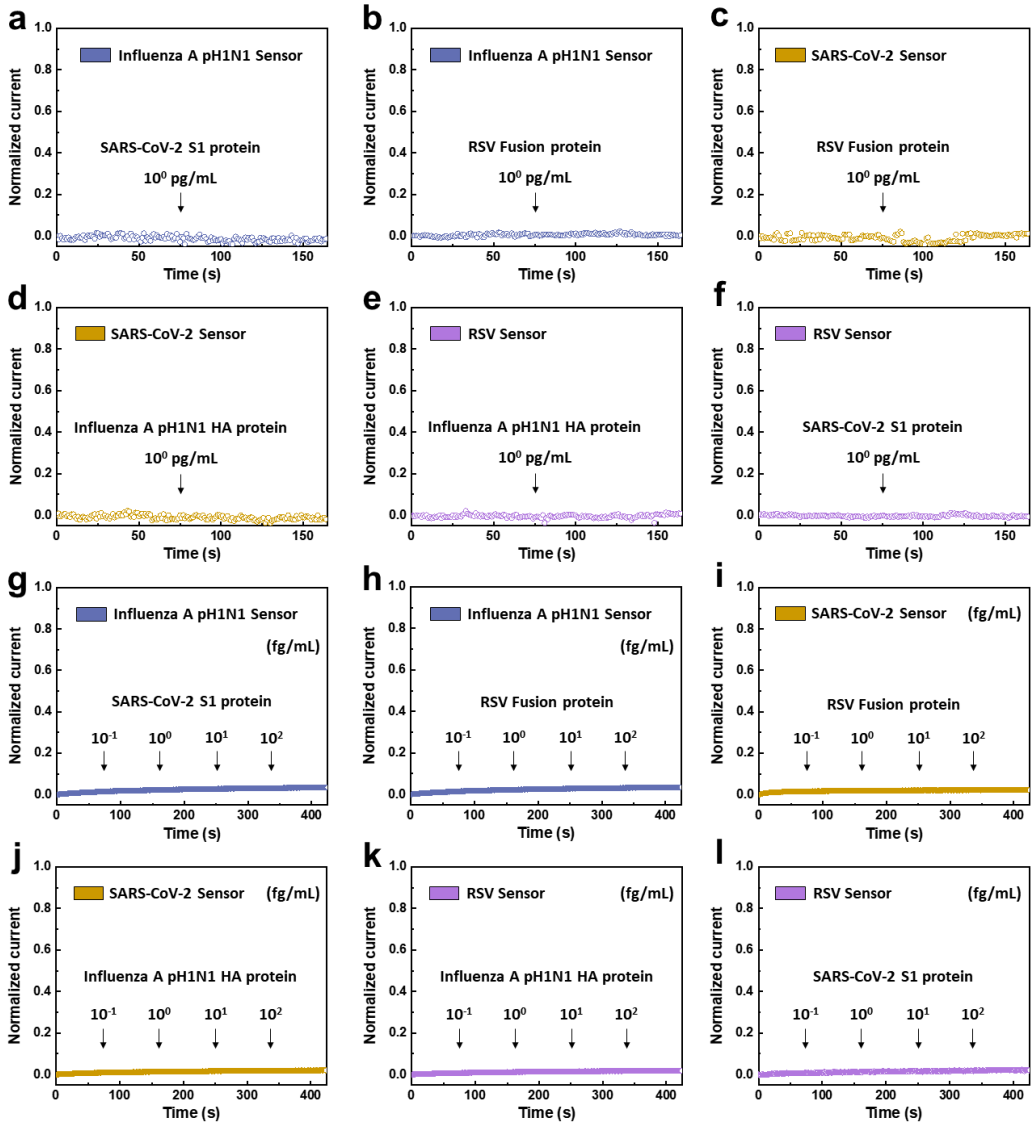

Figure S5. Normalized response variation of non-detected cases during cross-check with a (a–f) high concentration and (f–l) range of increasing concentrations of target proteins.

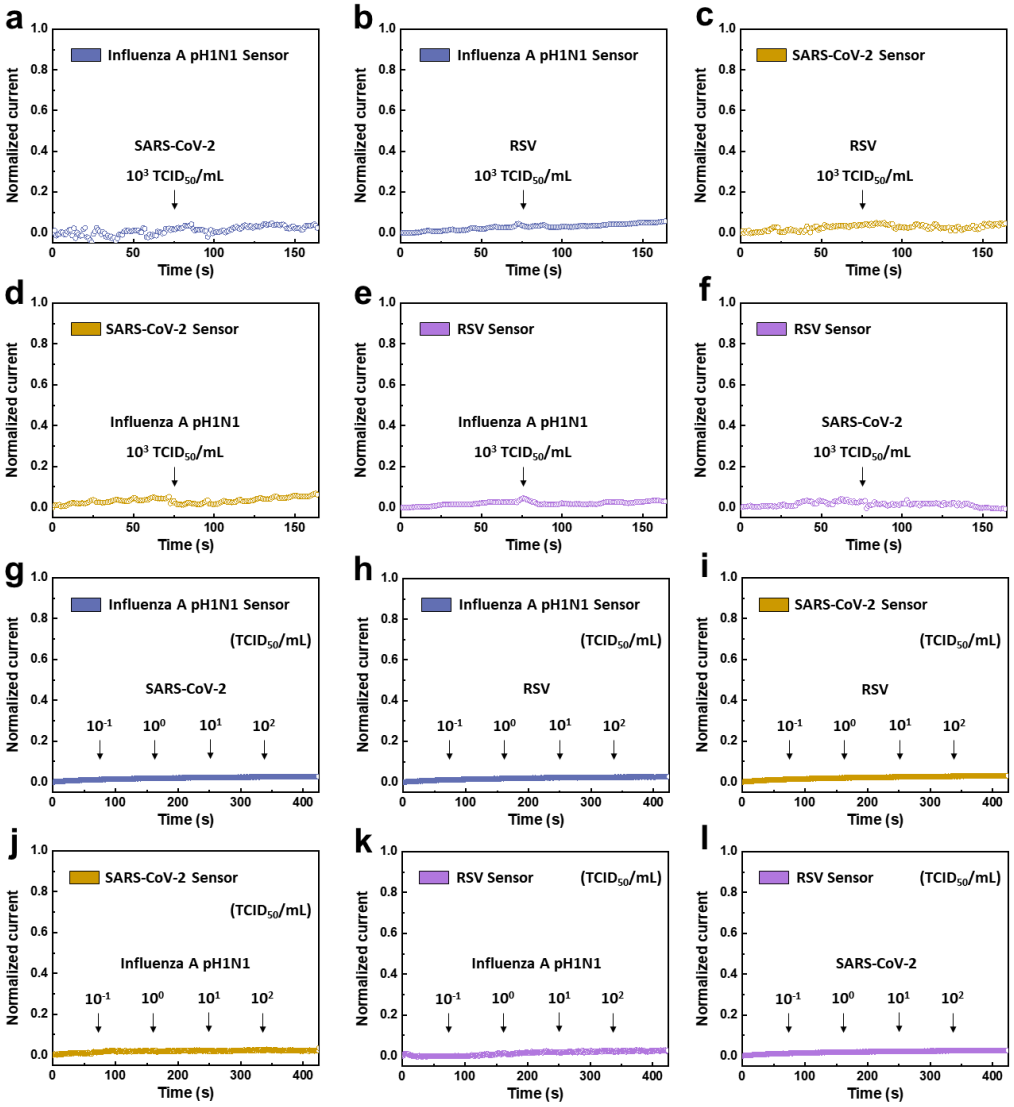

Figure S6 Normalized response variation of non-detected cases during a cross-check with a (a–f) high concentration and (f–l) range of increasing concentrations of cultured virus.

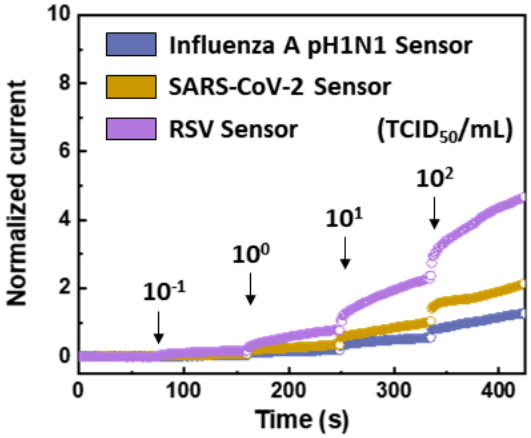

Figure S7. Normalized response variation during real-time detection of influenza A pH1N1, SARS-CoV-2, and RSV in artificial saliva mixture solution.

References

Fathi-Hafshejani, P., Azam, N., Wang, L., Kuroda, M.A., Hamilton, M.C., Hasim, S., Mahjouri-Samani, M., 2021. ACS Nano 15, 11461–11469.

Hideshima, S., Hayashi, H., Hinou, H., Nambuya, S., Kuroiwa, S., Nakanishi, T., Momma, T., Nishimura, S.I., Sakoda, Y., Osaka, T., 2019. Sci. Rep. 9.

Jang, H.J., Sui, X., Zhuang, W., Huang, X., Chen, M., Cai, X., Wang, Y., Ryu, B., Pu, H., Ankenbruck, N., Beavis, K., Huang, J., Chen, J., 2022. ACS Appl. Mater. Interfaces 14, 24187–24196.

Li, H., Yang, J., Wu, G., Weng, Z., Song, Y., Zhang, Yuxuan, Vanegas, J.A., Avery, L., Gao, Z., Sun, H., Chen, Y., Dieckhaus, K.D., Gao, X., Zhang, Yi, 2022. Angew. Chemie - Int. Ed. 61.

Li, Y., Peng, Z., Holl, N.J., Hassan, M.R., Pappas, J.M., Wei, C., Izadi, O.H., Wang, Y., Dong, X., Wang, C., Huang, Y.W., Kim, D., Wu, C., 2021. ACS Omega 6, 6643–6653.

Uhm, M., Lee, J.M., Lee, J., Lee, J.H., Choi, S., Park, B.G., Kim, D.M., Choi, S.J., Mo, H.S., Jeong, Y.J., Kim, D.H., 2019. Sensors (Switzerland) 19.

Zamzami, M.A., Rabbani, G., Ahmad, A., Basalah, A.A., Al-Sabban, W.H., Nate Ahn, S., Choudhry, H., 2022. Bioelectrochemistry 143, 107982.